2014 Fifth International Conference on Intelligent Systems, Modelling and Simulation

Analysis of Geometric, Zernike and United Moment Invariants Techniques Based on Intra-class Evaluation

Mohd Wafi Nasrudin[1*], Shahrul Nizam Yaakob[2],
Rozmie Razif Othman[3], Iszaidy Ismail[5,]
Mohd Ilman Jais[6],

School of Computer and Communication Engineering
Universiti Malaysia Perlis, Perlis, Malaysia
waffy88@yahoo.com[1], ysnizam@gmail.com[2],
rozmie@unimap.edu.my[3], iszaidyismail@gmail.com[5],
ilman_kun@gmail.com[6]

Aimi Salihah Abdul Nasir[4]

School of Mechatronic Engineering
Universiti Malaysia Perlis
Perlis, Malaysia
aimi_salihah@yahoo.com[4]

Abstract— In this paper, three moment invariants techniques have been used to extract the shape properties of the image. There are geometric moment, zernike moment and united moment invariants. These moment invariants have been used to analyze the image due to its invariant features of an image based on scaling factor and rotation. A set of equations known as intra-class analysis has been applied to measure the similarity of feature vector that represent the same object. The results obtained in this study have been analyzed and compared in terms of intra-class analysis in order to find the best technique among the three different types of moments. Based on the results that have been obtained by using the similar image, it is found that the geometric and united moment invariants techniques are better with small values of total percentage mean absolute error (TPMAE) as compared to zernike moment invariants.

Keywords-geometric moment invariant; zernike moment invariant; united moment invariant; shape analysis; intra-class analysis

I. INTRODUCTION

Shape analysis refers to the process of analyzing raw data and taking an action based on the classes of the shape. The major component in shape analysis is feature extraction which it is used for extracting the features in an image either the structural approach or global approach. Shape analysis is also a part of pattern recognition techniques which aims to extract the unique values from an object that differentiates it from the other objects. For example, in order to perform the face recognition, the feature extraction is used to retrieve the values that represent characteristics of the object. An object feature extraction can be done by various methods such as geometric moment invariant, united moment invariant and zernike moment invariant.

The geometric moment invariant (GMI) was first introduced by Hu in 1962 [1]. Hu introduced the seven functions using algebraic invariants [1]. This technique has been chosen to perform the feature extraction for image characteristics because the rotation scale translation (RST) invariant or characteristic produced by this method does not change the treatment of rotation, scaling and translation [2,5]. The united moment invariant (UMI) was introduced

by Yunan in 2003 [8]. The UMI is an extension of GMI that tends to reduce the effects of scaling factors in moment invariant function because of the affection of many factors. In UMI, the rotation, translation and scaling can be discretely kept invariant to region, closed and unclosed boundary. The calculation of UMI is quite similar to GMI. Meanwhile, the zernike moment invariant (ZMI) was produced by Teague in 1980 [10,12]. It is also called as zernike polynomials because it is based on continuous functions [9,11]. This method has been proposed to improve the conventional geometric invariants for rotation purposed.

Intra-class evaluation indicates the study done within the same group but under the influence of different scaling and rotations factors of the representing images [4,7]. A series of equations has been introduced to analyze between the original object with new various rotations and scale object by measuring the similarities between them. This evaluation can also be used to find the best technique among the various techniques within the same group[3].
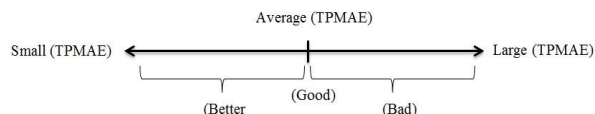
Figure 1.   Description of the intra-class

Fig. 1 represents the brief description of the intra-class. Based on Fig. 1, if the value of total percentage mean absolute error (TPMAE) is large, it means the technique is bad compared to the other techniques. And if the value of TPMAE is average, the technique is good. Meanwhile, if the value of TPMAE is small, the technique is better than other techniques.

II. THEORY OF MOMENT INVARIANTS

A. Geometric Moment Invariant

The geometric moment invariant (GMI) is used for a function. The order $(p+q)$ of $f(x, y)$ for GMI is defined in (1). Based on (1), p, q are the integer of $0,1,2,3.......$, x and y are the coordinate of the image and $x^p y^p$ is the basic function [5,6] .

$$m_{pq} = \int_{-\infty}^{\infty} \int_{-\infty}^{\infty} x^p y^q f(x,y) dx dy \qquad (1)$$

Equation (2) shows the general definition of an image in the size $M \times N$ pixels for digital image where $h(x,y)$ is a pixel value for an image of size $M \times N$.

$$m_{pq} = \sum_{x=1}^{N} \sum_{y=1}^{M} x^p y^q h(x,y) \qquad (2)$$

The central moments can be defined by substituting (3) and (4) into (5).

$$\bar{x} = m_{10} \div m_{00} \qquad (3)$$
$$\bar{y} = m_{01} \div m_{00} \qquad (4)$$
$$\mu_{pq} = \sum_{x=1}^{N} \sum_{y=1}^{M} (x - \bar{x})^p (y - \bar{y})^q h(x,y) \qquad (5)$$

Equation (6) is used to normalized the central moment in order to produce the invariant properties.

$$\eta_{pq} = \frac{\mu_{pq}}{\mu_{00}^{\frac{p+q+2}{2}}} \qquad (6)$$

The six functions of GMI can be determined from the normalized central moments and are shown in (7).

$$\phi_1 = (\eta_{20} + \eta_{02})$$
$$\phi_2 = (\eta_{20} - \eta_{02})^2 + 4\eta_{11}^2$$
$$\phi_3 = (\eta_{30} - 3\eta_{12})^2 + (3\eta_{21} - \eta_{03})^2$$
$$\phi_4 = (\eta_{30} + \eta_{12})^2 + (\eta_{21} + \eta_{03})^2$$
$$\phi_5 = (\eta_{30} - 3\eta_{12})(\eta_{30} + \eta_{12})[(\eta_{30} + \eta_{12})^2 - 3(\eta_{21} + \eta_{03})^2]$$
$$\quad + (3\eta_{21} + \eta_{03})(\eta_{21} + \eta_{03})[3(\eta_{30} + \eta_{12})^2 - (\eta_{12} + \eta_{03})^2]$$
$$\phi_6 = (\eta_{20} - \eta_{02})[(\eta_{30} + \eta_{12})^2 - (\eta_{21} + \eta_{03})^2] +$$
$$\quad 4\eta_{11}(\eta_{30} + \eta_{12})(\eta_{21} + \eta_{03}) \qquad (7)$$

B. United Moment Invariants

The calculations of UMI are quite similar to GMI. The definition of scaling equation normal, discrete and boundary as given in (8), (9), and (10) respectively are the three conditions that relate to GMI with the effect of scaling factors [8].

$$\eta_{pq} = \frac{\mu_{pq}}{\mu_{00}^{\frac{p+q+2}{2}}} \qquad (8)$$

$$\eta'_{pq} = \rho^{p+q} \eta_{pq} = \frac{\rho^{p+q} \mu_{pq}}{\mu_{00}^{\frac{p+q+2}{2}}} \qquad (9)$$

$$\eta''_{pq} = \frac{\mu_{pq}}{\mu_{00}^{p+q+1}} \qquad (10)$$

The six formulas for united moment invariants (UMI) are shown in (11).

$$\theta_1 = \sqrt{\phi_2} \div \phi_1 \qquad \theta_4 = \phi_5 \div (\phi_3 \times \phi_4)$$
$$\theta_2 = \phi_6 \div (\phi_1 \times \phi_4) \qquad \theta_5 = (\phi_1 \times \phi_6) \div (\phi_2 \phi_5)$$
$$\theta_3 = \sqrt{\phi_5} \div \phi_4 \qquad \theta_6 = ((\phi_1 + \sqrt{\phi_2})\phi_3) \div \phi_6 \qquad (11)$$

C. Zernike Moment Invariants

Zernike moment has been introduced based on a continuing orthogonal function called Zernike polynomials. The zernike moment from a digital image can be computed by using (12) [13,14]. The value of $f(x,y)$ is referring to the pixel density $M \times N$ image size.

$$Z_{mn} = \frac{n+1}{\pi} \sum_{k=m}^{n} B_{nmk} \sum_{x=1}^{N} \sum_{y=1}^{M} (x - iy)^m (x^2 + y^2)^{(k-m)/2} f(x,y) \qquad (12)$$

Where

$$B_{nmk} = \frac{(-1)^{(n-k)2} \left(\frac{n+k}{2}\right)!}{\left(\frac{n-k}{2}\right)! \left(\frac{k+m}{2}\right)! \left(\frac{k-m}{2}\right)!} \qquad (13)$$

The equations for zernike and geometric moments for rotation and scaling factors can be derived from (12) by substituting from (13). Thus, the magnitude $|Zmn|$ of the zernike moment can be taken as a rotation invariant feature of the underlying image function as (14) [7].

$$Z_{20} = \left(\frac{3}{\pi}\right)(2(\eta_{20} + \eta_{02}) - \eta_{00})$$

$$|Z_{22}|^2 = \left(\frac{3}{\pi}\right)^2 [(\eta_{20} - \eta_{02})^2 + 4\eta_{11}^2]$$

$$|Z_{31}|^2 = \left(\frac{12}{\pi}\right)^2 [(\eta_{30} + \eta_{12})^2 + (\eta_{03} + \eta_{21})^2]$$

$$|Z_{33}|^2 = \left(\frac{4}{\pi}\right)^2 [(\eta_{30} - \eta_{12})^2 + (\eta_{03} - \eta_{21})^2]$$

$$|Z_{42}|^2 = \left(\frac{5}{\pi}\right)^2 ([4(\eta_{40} - \eta_{04}) - 3(\eta_{20} - \eta_{02})]^2 + [6\eta_{11} - 8(\eta_{31} - \eta_{13})]^2)$$

$$Z_{40} = \left(\frac{5}{\pi}\right)(\eta_{00} - 6(\eta_{20} + \eta_{02}) + 6(\eta_{40} + \eta_{04} + 2\eta_{22})) \qquad (14)$$

III. EXPERIMENTATION

In this study, the selected image has been used to get the range of the invariant. The image that has been used for the analysis is shown in Fig. 3. This image has been resized into the standard size of 800×600 pixels. Before the image has been resize into the standard size, the image has been converted into a binary level as shown in Fig. 2. This process is performed in order to ease the extraction of feature image as the pixels of the image region are assigned a value of one and the rest are as assigned as zero. Then, each image will illustrate into various rotations and scale as shown in Table I.

TABLE I.   DIFFERENT ORIENTATION OF IMAGE

No.	Image Orientation
a	Original image
b	Image resized to half of the original image
c	Image rotated to 45°
d	Image resized to half of the original image and rotated to 45°
e	Image enlarged 1.5X and rotated to 20°

Figure 2.   The result of binary image

Figure 3.   Binary image with difference scaling and rotation : (a) Original image, (b) Image resized to half of the original image, (c) Image rotated to 45°, (d) Image resized to half of the original image and rotated to 45°, (e) Image enlarged 1.5X and rotated to 20°

Then, features vectors are computed by using the three moment invariants as mentioned previously. In order to find the best result, an intra-class analysis which are based on the shape and rotation have been used. Intra-class analysis is the process that defines the similar images with the smallest value of TPMAE. The series of equations that are used to measure the invariant characteristics can be described as follows:

$$AE_m^a(\gamma_i) = \Delta_m^a \gamma_i = \left| H_a(\gamma_i) - F_m^a(\gamma_i) \right| \quad (15)$$

$$PAE_m^a(\gamma_i) = \%\Delta_m^a \gamma_i = \frac{\Delta_m^a \gamma_i}{\left| H_a(\gamma_i) \right|} \times 100 \quad (16)$$

$$PMAE1_m^a(\gamma) = \frac{1}{I} \sum_{i=1}^{I} PAE_m^a(\gamma_i) \quad (17)$$

$$PMAE2^a(\gamma_i) = \frac{1}{M} \sum_{m=1}^{M} PAE_m^a(\gamma_i) \quad (18)$$

$$TPMAE_a = \frac{1}{M} \sum_{m=1}^{M} PMAE1_m^a(\gamma) \quad (19)$$

By using the equations for intra-class analysis, the value of absolute error (AE), percentage absolute error (PAE), percentage mean absolute error (PMAE) and total percentage mean absolute error (TPMAE) of the image class are computed. For this analysis, the values of AE, PAE, PMAE and TPMAE for each dimension are calculated by using (15) until (19).

IV.   RESULTS AND DISCUSSIONS

This section describes the sets of feature vectors that have been produced by the three types of moment invariants and intra-class analysis in order to find the best type of moment that can give the significant results. The six elements of moment invariants of each method have been computed to find feature vectors. Tables II, III and IV tabulated the feature vectors that have been produced by these three moment invariant techniques. From the table, it can be seen that a dissimilar of feature vectors have been produced due to different moment techniques that have been used.

TABLE II.   GEOMETRIC MOMENT INVARIANT feature vector

	Ø1	Ø2	Ø3	Ø4	Ø5	Ø6
Original	0.62941	2.31291	2.77268	4.69138	8.44142	5.85095
0.5X	0.62649	2.30470	2.76771	4.71752	8.48079	5.87327
45	0.62918	2.31334	2.77090	4.69204	8.44222	5.85211
0.5X+45	0.62633	2.30392	2.77240	4.73194	8.50307	5.88667
1.5X+20	0.62806	2.30830	2.77017	4.70065	8.45512	5.85804

TABLE III.   UNITED MOMENT INVARIANT FEATURE VECTOR

	Θ1	Θ2	Θ3	Θ4	Θ5	Θ6
Original	2.44561	2.01407	0.61941	0.65580	0.57558	1.00087
0.5X	2.45179	2.01866	0.61670	0.65607	0.57928	0.99124
45	2.44478	2.01357	0.62015	0.65575	0.57442	1.00334
0.5X+45	2.45315	2.02036	0.61780	0.65728	0.57813	0.99251
1.5X+20	2.44883	2.01737	0.61871	0.65627	0.57672	0.99720

TABLE IV.   ZERNIKE MOMENT INVARIANT FEATURE VECTOR

	Z20	Z22	Z31	Z33	Z40	Z42
Original	-0.3058	2.32267	3.52021	2.53068	-0.3891	1.31015
0.5X	-0.3085	2.31336	3.55551	2.52610	-0.3896	1.29663
45	-0.3054	2.32458	3.50915	2.53094	-0.4589	1.57069
0.5X+45	-0.3084	2.31665	3.54211	2.52306	-0.4617	1.57093
1.5X+20	-0.3073	2.31754	3.52944	2.52794	-0.4542	1.67834

In this study, AE were used to compute the invariant characteristic of feature vectors. This is because AE can define the difference between an original data with new data. Table V and VI have shown the AE and PAE for the image with 45° and different types of moment. The number on the top column in the table refers to the feature dimension and it can be seen clearly the advantage of PAE against the AE. For example, it can be seen the AE for GMI at the first dimension is smaller than UMI. But when PAE is tabulated in Table VI, the PAE for UMI is smaller than GMI. Based on this, the UMI is more invariant as compared to GMI. Nevertheless, PAE is not bringing a lot of information needed because PAE is used in the analysis performance moment techniques under difference perturbations.

TABLE V. AE FOR IMAGE WITH 45° AND DIFFERENT TYPES OF MOMENT

	1	2	3	4	5	6
GMI	0.00023	0.0004	0.00177	0.00066	0.0007	0.0011
UMI	0.00082	0.0005	0.00073	0.00005	0.0011	0.0024
ZMI	0.00043	0.0019	0.01106	0.00026	0.0697	0.2605

TABLE VI. PAE FOR IMAGE WITH 45° AND DIFFERENT TYPES OF MOMENT

	1	2	3	4	5	6
GMI	0.03766	0.0185	0.06412	0.01410	0.0094	0.0197
UMI	0.03383	0.0248	0.11882	0.00851	0.2030	0.2472
ZMI	0.14255	0.0825	0.31425	0.01037	17.928	19.886
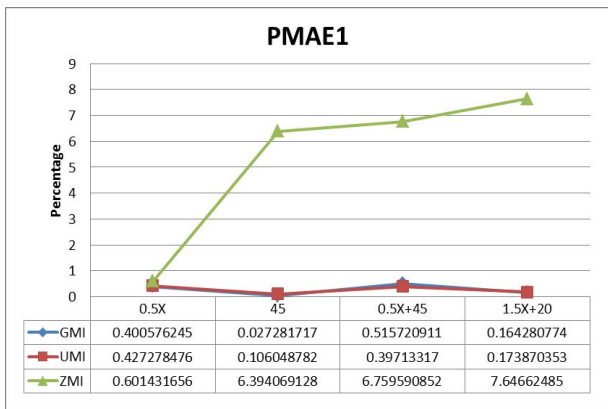
Figure 4. Graph of percentage mean absolute error (PMAE1)

Fig. 4 shows the graph of PMAE1 that has been computed by using (17). There are two types of PMAE for this analysis which are PMAE1 and PMAE2. The goal of PMAE1 is to calculate the error occurred in one object among difference variations. The graph in Fig. 4 demonstrates the value of PMAE1 versus image variation. It describes the ZMI generates the highest error among other moments.
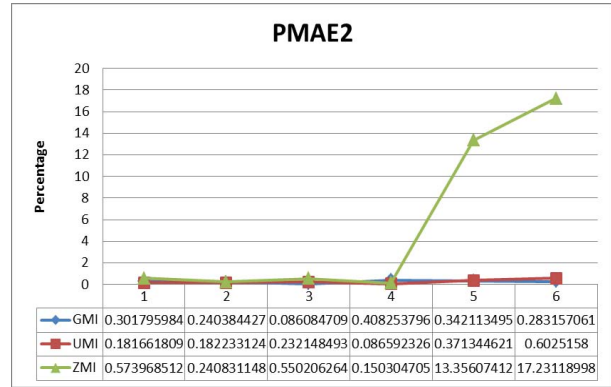
Figure 5. Graph of percentage mean absolute error (PMAE2)

The results of PMAE2 that have been obtained by calculating using (18) are shown in Fig. 5. The advantage of using the PMAE2 is it can determine the error scattering within the dimension of feature vectors. From the graph, it can be seen the GMI and UMI produced smaller error as compared to ZMI.
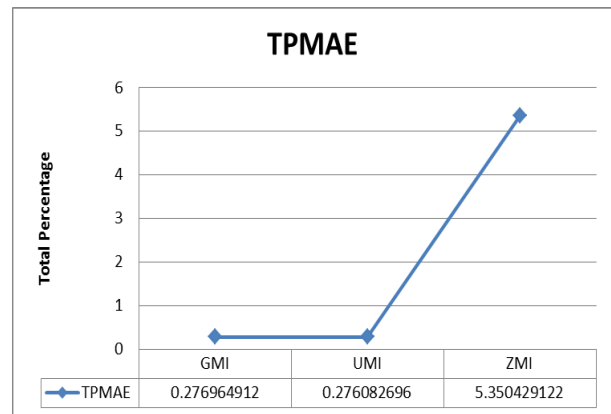
Figure 6. Total Percentage Min Absolute Error (TPMAE)

Meanwhile, Fig. 6 represents the graph of total percentage min absolute error. The TPMAE can be computed from either PMAE1 or PMAE2 because it will produce the similar result. The TPMAE is a final process to detect the error for an image of different types of moment. From the graph, it can be seen that ZMI has produced higher error as compared to GMI and UMI.

V. CONCLUSIONS

In this paper, the feature vectors that were received from three different types of moment invariant have been computed for shape analysis in order to identify the technique that has the smallest error or better with others method by using intra-class analysis. For the feature extraction of three techniques is no problem where is all methods can be used to perform feature extraction of a digital image that is able to distinguish the characteristics of the image even if this image made changes rotation scale

translation (RST). It can be concluded that the geometric and united moments are better than zernike moment based on the intra-class analysis. This has been proven based on the results in Fig. 5 for where the graph shows that the zernike moment has produced the highest TPMAE values as compared to the geometric and united moments invariants.

REFERENCES

[1] M. K. Hu, "Visual pattern recognition by moments invariants," IRE Trans. Information Theory, 8, 1962, pp. 179-187.

[2] S. Maitra, "Moment invariants," Proc. of the IEEE, vol. 67, 1979, pp. 697–699.

[3] S. N. Yaakob, P. Saad, and M. F. Jamlos, "On Analysis of Invariant Characteristic for Moment Invariant Techniques," Journal of Engineering Research & Education, vol. 3, (2006) pp. 29-42.

[4] S. N. Yaakob, P. Saad and A.H. Abdullah, "Insert recognition using fuzzy ARTMAP," Proc. Intl. Conf. Robotics, Vision, Information and Signal Processing ROVISP , 2005, pp. 679-684.

[5] M. Rizon, H. Yazid, P. Saad, A. Y. M. Shakaff, A.R. Saad, M.R. Mamat, S. Yaacob, H. Desa and M. Karthigayan, "Object Detection using geometric invariant moment," American Journal of Applied Sciences, vol. 6, 2006, pp. 1876-1878.

[6] Belkasim, S. O. Shridhar and M. Ahmadi, "Pattern Recognition with Moment Invariants, A Comparative Study and New Results," Pattern Recognition, vol. 24, no. 12, 1991, pp. 1117-1138.

[7] P. Saad, "Feature extraction of trademark images using geometric invariant moment and zernike moment comparison," Chiang Mai J. Sci., 31, 2004, pp 217-222.

[8] S. Yinan, L. Weijun and W. Yuechao, "United moment invariants for shape discrimination," IEEE Proceedings on International Conference on Robotics, Intelligent Systems and Signal processing, vol 1, 2003, pp. 88–93.

[9] S. K. Hwang and W. Y. Kim, "A novel approach to the fast computation of Zernike moments," Pattern Recognition, 39, 2006, pp 2065–2076.

[10] A. Khotanzad, H. Yaw Hua, "Invariant image Recognition by Zernike moments," IEEE Transactions on Pattern Analysis and Machine Intelligence, Vol. 12, May 1990, pp. 489 497.

[11] J. Hanjie and Z. Hongqing, "Degraded image analysis using Zernike moment invariants," in Acoustics, Speech and Signal Processing, 2009. ICASSP 2009. IEEE International Conference on, 2009, pp. 1941-1944.

[12] Khotanzad and H. Y. Hua, "Rotation invariant pattern recognition using Zernike moments," in Pattern Recognition, 9th International Conference on, 1988, vol.1, pp. 326-328.

[13] Z. Hui, D. Zhifang, and S. Huazhong, "Object recognition by a complete set of pseudo-Zernike moment invariants," in Acoustics Speech and Signal Processing (ICASSP), 2010 IEEE International Conference on, 2010, pp. 930-933.

[14] S. J. Perantonis and P. J. G. Lisboa, "Translation, rotation, and scale invariant pattern recognition by high-order neural networks and moment classifiers," Neural Networks, IEEE Transactions on, vol. 3, 1992, pp. 241-251.